Acta metall. Vol. 30, pp. 447 to 455, 1982
Printed in Great Britain

0001-6160/82/020447-09$03.00/0
Pergamon Press Ltd

STRAIN LOCALIZATION IN AMORPHOUS METALS

P. S. STEIF, F. SPAEPEN and J. W. HUTCHINSON
Division of Applied Sciences, Harvard University, Cambridge, MA 02138, U.S.A.

(*Received* 25 *June* 1981)

Abstract—Inhomogeneous flow in metallic glasses is studied in this paper within the context of continuum mechanics. Motivated by similar work for elastic–plastic solids, the possibility of strain localization into a shear band is investigated for a metallic glass which is modelled as a nonlinear viscoelastic solid. The essential features of the localization problem are brought out through an analysis of the constitutive law which reveals a catastrophic softening via free volume creation. Analytic expressions for the stress at catastrophic softening agree very closely with the stress at strain localization calculated from the numerical solution of the full set of shear band equations.

Résumé—Nous étudions dans cet article l'écoulement hétérogène dans les verres métalliques, dans le cadre de la mécanique des milieux continus. Poussés par des travaux analogues dans les solides élastiques–plastiques, nous avons envisagé la possibilité d'une localisation de la déformation dans une bande de cisaillement d'un verre métallique, représenté par un solide visco-élastique non linéaire. Les traits essentiels du problème de cette localisation sont pris en compte par une analyse de la loi de constitution qui révèle un adoucissement catastrophique par l'intermédiaire de la création d'un volume libre. Les expressions analytiques de la contrainte pour l'adoucissement catastrophique sont très proches de la contrainte à la localisation de la déformation que l'on calcule en résolvant numériquement l'ensemble complet des équations des bandes de cisaillement.

Zusammenfassung—In dieser Arbeit wird das inhomogene Fließen metallischer Gläser im Rahmen der Kontinuumsmechanik behandelt. Angeregt von ähnlichen Arbeiten an elastisch–plastischen Festkörpern wird in der Näherung eines nichtlinearen viskoelastischen Festkörpers untersucht, ob die Verformung sich in metallischen Gläsern in einem Scherband lokalisieren kann. Die wesentlichen Eigenschaften dieses Lokalisierungsproblems werden mit einer Analyse der Grundgleichungen ermittelt; es ergibt sich eine katastrophale Entfestigung durch die Erzeugung freien Volumens. Die analytischen Ausdrücke für die Spannung bei dieser katastrophalen Entfestigung stimmen sehr gut mit der Spannung bei der Lokalisierung der Dehnung überein, welche mit dem vollständigen Satz der Scherbandgleichungen numerisch berechnet wirde.

1. INTRODUCTION

In recent years, the need for a more fundamental understanding of flow in metallic glasses has motivated a variety of experimental investigations: mapping out flow regimes [1, 2], evaluating temperature and strain-rate sensitivities [2–4], and assessing the dependence of flow on microstructure and heat treatment [5–7]. Theoretical models have been put forth concurrently and have helped to explain various features of flow, particularly in the homogeneous regime [1, 4, 8–11].

Relatively less has been established concerning inhomogeneous flow. In particular, little is understood about the embrittlement with annealing of metallic glasses that are otherwise ductile and flow at higher stresses by the formation of a shear band [10, 12]. Investigating strain localization alone seems to be a first step in approaching the problem of inhomogeneous flow. Argon [11] has shown that flow can localize in a band in which the strain rate has been perturbed, when the threshold stress for driving the local shear transformations is altered through the creation of free volume. He used the stress exponent for steady-state flow governed by a microscopic shear transformation analogous to the formation of a dislocation loop. The free volume creation parameter was chosen independently of this transformation.

The present work is a more extensive treatment of strain localization using a simpler and more self-contained constitutive model proposed by Spaepen [1]. The shear band analysis takes full account of the transient nature of free volume creation and no assumptions are made as to the existence of a steady-state. Analytic formulae are derived for the stress at localization in terms of physical parameters such as the elastic shear modulus, initial free volume, and applied strain-rate.

2. PHENOMENOLOGY OF FLOW REGIMES IN METALLIC GLASSES

The phenomenology of the various flow regimes in amorphous metals has been the subject of several extensive reviews [1, 8, 10, 13, 14]. The standard mechanical test involves pulling a narrow rectangular

strip in tension. In the range in which the material can be considered a solid, essentially two deformation modes can be distinguished: homogeneous flow and inhomogeneous flow.

Homogeneous flow occurs at low stresses and high temperatures. Flow takes place uniformly with each volume element contributing an equal amount of strain. At lower stresses, the strain-rate increases linearly with stress; at slightly higher stresses the strain-rate follows the sinh (stress) law [4]. Fracture occurs when some section has necked down to a narrow thickness.

Inhomogeneous flow is observed at high stresses and low temperatures. The flow is localized in a thin band oriented at a 45° angle with tensile axis. The stress is very insensitive to strain-rate and temperature. Intense shear strains in the band decrease the load bearing cross-section, and fracture occurs *along* the plane of the shear band. The mechanism of fracture is a Taylor instability as evidenced by the typical vein-like pattern on the fracture surface [15, 16]. The localization of deformation into a shear band, as well as the occurrence of fracture by the Taylor instability along the plane containing the shear band and not along the plane of maximum normal stress, suggests that a softening of the material has taken place. Differential etching of the shear band indicates chemical changes, which supports the conjecture of a local softening [17]. Spaepen and Turnbull [18] have suggested that a local stress concentrator such as an edge crack may provide the softening needed to initiate the shear band. They calculate the effect of the dilatation on the viscosity at the point of the near-crack stress field where the theoretical strength is reached and conclude that the softening is substantial at least locally.

3. CONSTITUTIVE LAWS

Constitutive equations proposed by Spaepen [1], valid for homogeneous and inhomogeneous deformation, are employed. The equations model flow as occurring as a result of many microscopic rearrangements each contributing a small local shearing deformation. In general, the macroscopic shear strain-rate, $\dot{\gamma}$, is given by the following product

$\dot{\gamma}$ = (strain produced at each jump site) × (fraction of potential jump sites) × (net number of forward jumps at each site per second) (1)

In [1] the shear strain at each potential jump site is assumed to be 1. A potential site is a region in which the free volume (a measure of the departure from the ideally ordered structure) is greater than some critical volume (the effective hard-sphere volume of an atom, for example). Such an amount of free volume would allow the atoms participating in the rearrangement leading to the local shear strain to 'get by' one another. The atom fraction of potential sites can be calculated from the free volume theory of Turnbull and Cohen [19–21] as follows. Since in an amorphous metal the free volume is distributed statistically among all atoms, one can use fluctuation theory to calculate the probability that any one atom has about it a free volume greater than the critical volume. The fraction of potential jump sites is equal to that probability, therefore

the fraction of potential jump sites

$$= \exp\left[-\frac{\alpha v^*}{\bar{v}_f}\right] \tag{2}$$

where α is a geometrical factor of order 1, v^* is the critical (hard-sphere) volume, and $\bar{v}_f$ is the average free volume per atom. Throughout this paper, when dimensional and nondimensional quantities are to be distinguished, barred quantities will be dimensional. Also, the notation follows that of Spaepen [1] as closely as possible.

The net forward jump rate may be calculated from simple rate theory. In the absence of an applied shear stress, the numbers of forward and backward jumps coincide (no net shear accumulates), and the number of successful jumps in an unbiased system per second

$$= \nu \exp\left[-\frac{\Delta G^m}{kT}\right] \tag{3}$$

where ν is the frequency of atomic vibration and ΔG^m is the activation energy. In the presence of an applied shear stress the system is biased. The stress working through the local shear strain allows the system to lower its potential energy, whereas accomplishing a shear strain against an opposing shear stress requires an increase in potential energy. This biasing results in an extra factor in equation (3), hence the net rate of forward jumps in a biased system

$$= 2\nu \exp\left[-\frac{\Delta G^m}{kT}\right]\sinh\left(\frac{\bar{\tau}\Omega}{2kT}\right) \tag{4}$$

where Ω is the atomic volume and $\bar{\tau}$ is the shear stress.

Therefore, the irreversible (viscous) part of the strain-rate can be represented by the following general flow equation

$$\dot{\gamma}^p = 2\nu \exp\left[-\frac{\alpha v^*}{\bar{v}_f}\right]\exp\left[-\frac{\Delta G^m}{kT}\right]\sinh\left(\frac{\bar{\tau}\Omega}{2kT}\right) \tag{5}$$

A stress dependent viscosity η may be defined as follows:

$$\eta \equiv \frac{\bar{\tau}}{\dot{\gamma}^p} = \frac{\bar{\tau}}{2\nu \sinh\left(\frac{\bar{\tau}\Omega}{2kT}\right)}\exp\left[\frac{\alpha v^*}{\bar{v}_f}\right]\exp\left[\frac{\Delta G^m}{kT}\right] \tag{6}$$

Varying the free volume $\bar{v}_f$ can radically change the viscosity. As will become evident, the softening induced by increasing the free volume permits the localized deformation pattern which distinguishes inhomogeneous from homogeneous flow.

At low stresses, typical of homogeneous flow, the free volume is fixed and is representative of that in the liquid at the glass transition temperature. As mentioned above, inhomogeneous flow differs from homogeneous flow by the presence of severe strains concentrated in a few narrow bands of material which has undergone a structural change. Polk and Turnbull [22] suggested that the structural change is a process of strain-disordering. This concept has been extended and quantified by Spaepen [1] who also included a reordering process. In Spaepen's model, the free volume is the measure of disorder in the system. Free volume can be created (disordering) by the shear stress squeezing an atom into a hole smaller than itself; free volume can be annihilated (reordering) by a series of atomic jumps similar to those that allow a sample to relax towards metastable equilibrium during annealing. The net rate of increase of free volume, i.e. the difference between the amount created and the amount annihilated per unit time, is

$$\dot{\bar{v}}_f = v^* \nu \exp\left[-\frac{\alpha v^*}{\bar{v}_f}\right]\exp\left[-\frac{\Delta G^m}{kT}\right] \times \left\{\frac{2\alpha kT}{\bar{v}_f \bar{S}}\left(\cosh\frac{\bar{\tau}\Omega}{2kT} - 1\right) - \frac{1}{n_D}\right\} \tag{7}$$

where n_D is the number of atomic jumps needed to annihilate a free volume equal to v^*, and

$$\bar{S} = \tfrac{2}{3}\bar{G}\frac{(1+\sigma)}{(1-\sigma)},$$

where $\bar{G}$ is the shear modulus, and σ is Poisson's ratio.

In Section 5, results will be presented of an examination of strain localization in a viscous material modelled by the constitutive equations discussed above. As mentioned in the Introduction, it has been suggested that the shear band is initiated by microcracks (or other suitable stress raisers) which cause a local softening which propagates rapidly as deformation proceeds. But for time-independent plastic solids, much insight into localization phenomena has been gained by analyzing the mechanics of a body containing a material imperfection in the form of a band of slightly weaker material. In the same spirit, a shear band analysis of the present nonlinear visco-elastic solid will be carried out.

Prior to the shear band analysis, however, the uniform shearing of a homogeneous body modelled by the constitutive equations (5) and (7) is considered. The uniform shearing isolates the constitutive behavior from the kinematic effects of non-uniform deformation associated with a shear band. The strongly nonlinear character of the constitutive law, in particular the differential equation governing free volume creation, equation (7), permits a catastrophic softening to occur in the uniformly shearing body. The simplicity of the uniform deformation allows explicit expressions to be derived for the stress at which catastrophic softening occurs. Upon comparison with the shear band analysis, the stress at catastrophic softening will be seen to coincide with the stress at the onset of strain localization in an identical sample with a thin band of slightly weaker material. Therefore, the creation of free volume, with the attendant catastrophic softening, plays the central role in strain localization.

4. ONSET OF CATASTROPHIC SOFTENING IN UNIFORMLY SHEARING BODY

In addition to equation (7), the equation modelling a solid undergoing homogeneous shearing is

$$\frac{\dot{\bar{\tau}}}{\bar{G}} + 2\nu \exp\left[-\frac{\alpha v^*}{\bar{v}_f}\right]\exp\left[-\frac{\Delta G^m}{kT}\right]\sinh\left(\frac{\bar{\tau}\Omega}{2kT}\right) = \dot{\gamma} \tag{8}$$

Equation (8) states that the total strain-rate, $\dot{\gamma}$, is the sum of the elastic strain-rate and the viscous strain-rate. In what follows, the total strain-rate is regarded as a prescribed constant over the deformation history.

It is convenient to introduce the following dimensionless variables

$$v_f = \bar{v}_f/\alpha v^*, \qquad \tau = \bar{\tau}\Omega/2kT$$

$$t = R\bar{t}, \qquad G = \bar{G}\Omega/2kT$$

where

$$R = \nu \exp\left[-\frac{\Delta G^m}{kT}\right].$$

Then equations (7) and (8) become

$$\alpha v_f' = e^{-1/v_f}\left[\frac{\cosh\tau - 1}{G\beta v_f} - \frac{1}{n_D}\right] \tag{9}$$

$$\frac{\tau'}{G} + 2e^{-1/v_f}\sinh\tau = \gamma' \tag{10}$$

where

$$\beta = \frac{2}{3}\frac{(1+\sigma)}{(1-\sigma)}\frac{v^*}{\Omega}$$

and $(\,)'$ denotes differentiation with respect to t. At $t = 0$, τ and v_f are taken to have their initial values $\tau = 0$, and $v_f = v_i$. As mentioned, γ' is taken to be constant.

In order to follow the variation of stress and free volume with time in a sample subjected to a given applied strain-rate, equations (9) and (10) were integrated numerically for various values of γ', G, and v_i. For all values of the parameters, the curve of stress as a function of total strain is qualitatively similar to Fig. 1. An initial elastic response is followed by a precipitous drop in stress during which the creep

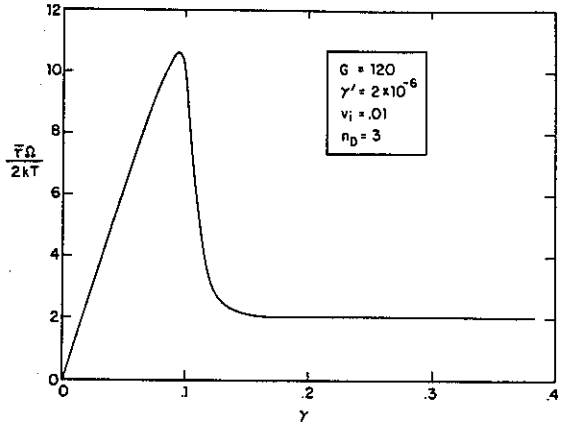

Fig. 1. Example of a stress–strain curve for a uniformly shearing body under constant strain-rate.

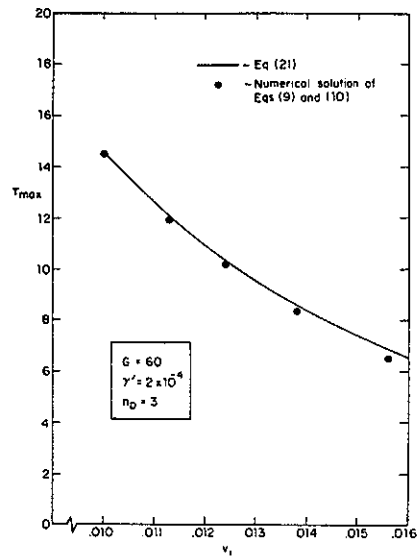

Fig. 3. Comparison of the nondimensional maximum stress as given by the numerical solution of equations (9) and (10) with their approximate solution equation (21) for various values of the nondimensional initial free volume v_i.

strain-rate increases by many orders of magnitude. (For strains larger than 0.15, the curve in Fig. 1 indicates that a steady state stress has been achieved at which the free volume and viscosity stay constant. That the maximum stress is 5 or 6 times the steady state stress will be of interest later.) It is noted that the maximum stress immediately precedes the precipitous drop in stress. The points in Figs 2–4 show the dependence of the maximum stress τ_{max} on various essential parameters.

An approximate, but accurate, formula for τ_{max} is now obtained by integrating an appropriately modified version of equation (9). Since $\tau = \tau_{max}$ at $\tau' = 0$, equation (10) implies that τ_{max} satisfies

$$2e^{-1/v_f} \sinh \tau_{max} = \gamma' \tag{11}$$

One can rewrite equation (9) in the form

$$\alpha \frac{dv_f}{d\tau} \tau' = e^{-1/v_f} \left[\frac{\cosh \tau - 1}{G\beta v_f} - \frac{1}{n_D} \right] \tag{12}$$

It is evident from Fig. 1 that before the first peak the stress is linear with strain except in the immediate vicinity of the maximum. That is, nonlinearities in the constitutive law are so strong that an essentially linear elastic response is followed immediately by such a drastic decrease in viscosity that the stress falls

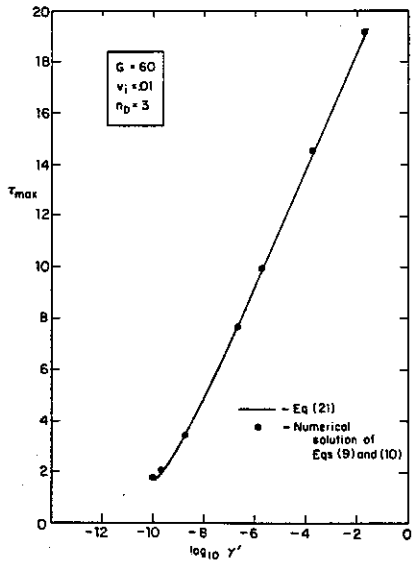

Fig. 2. Comparison of the nondimensional maximum stress as given by the numerical solution of equations (9) and (10) with their approximate solution equation (21) for various values of the nondimensional strain rate γ'.

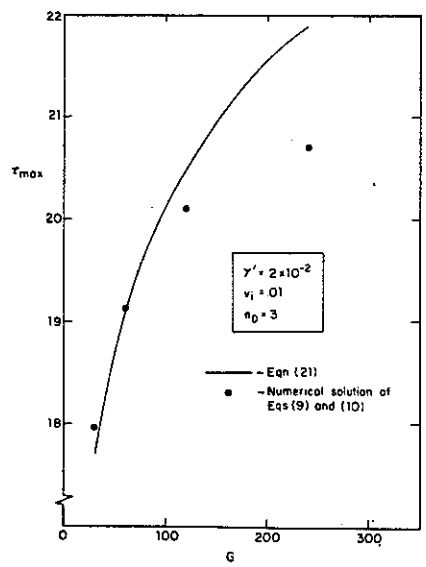

Fig. 4. Comparison of the nondimensional maximum stress as given by the numerical solution of equations (9) and (10) with their approximate solution equation (21) for various values of the nondimensional shear modulus G.

off precipitously. Therefore, to allow equation (12) to be integrated in closed form, an acceptable approximation is to let $\tau' = G\gamma'$ in equation (12) prior to attaining the maximum stress, even though the condition for the maximum is $\tau' = 0$.

Finally, annihilation is taken into account approximately. Completely neglecting

$$\frac{1}{n_D} \text{ in comparison with } \frac{\cosh\tau - 1}{G\beta v_f}$$

would rule out annihilation altogether and permit the system to create free volume at even the lowest stresses. (Furthermore, the annihilation of free volume must play a key role in determining the steady state. Results to be presented later on the localization problem indicate, however, that the steady state may never be attained.) The approximation is to neglect the term $1/n_D$ in equation (12) but to integrate the right hand side from $\tau = \tau_0$ (instead of $\tau = 0$) where τ_0 is the stress at which creation would first exceed annihilation. While the assumption of

$$\frac{\cosh\tau - 1}{G\beta v_f} \gg \frac{1}{n_D}$$

is poor for τ less than 1, little damage is done to the calculation of free volume. This is true primarily because the exponential term in equation (12) is much smaller initially at lower free volumes than later at higher free volumes. τ_0 satisfies

$$\cosh\tau_0 = 1 + \frac{G\beta v_i}{n_D} \tag{13}$$

With the above assumptions, equation (12) can be approximated by

$$G\gamma'\alpha\frac{dv_f}{d\tau} = e^{-1/v_f}\left[\frac{\cosh\tau - 1}{G\beta v_f}\right] \tag{14}$$

Applying the limits of integration as specified above, one can arrange equation (14) in the form

$$\int_{v_i}^{v_f} G^2\beta\alpha\gamma' v e^{1/v}\,dv = \int_{\tau_0}^{\tau}(\cosh x - 1)\,dx \tag{15}$$

where v_f is the current value of the free volume.

This can be integrated exactly [23], to give

$$\tfrac{1}{2}G^2\beta\alpha\gamma'\{v_f e^{1/v_f}(v_f + 1) - v_i e^{1/v_i}(v_i + 1) - [Ei(1/v_f) - Ei(1/v_i)]\} = \sinh\tau - \tau - (\sinh\tau_0 - \tau_0) \tag{16}$$

where $Ei(z)$ is the exponential integral function defined as [24]

$$-Ei(-z) = \int_z^\infty \frac{e^{-t}}{t}\,dt \tag{17}$$

Since the arguments of $Ei(z)$ in equation (16) are large ($0.04 < v < 0.07$), $Ei(z)$ may be replaced by its asymptotic expansion for large z [25], allowing equation (16) to be rewritten as

$$G^2\beta\alpha\gamma'[v_i^3 e^{1/v_i} - v_f^3 e^{1/v_f}] = \sinh\tau - \tau - (\sinh\tau_0 - \tau_0) \tag{18}$$

Equation (11), rearranged in the form

$$e^{1/v_f} = \frac{2\sinh\tau_{max}}{\gamma'} \tag{19}$$

is now imposed on equation (18).

The maximum stress satisfies

$$G^2\beta\alpha\gamma' v_i^3 e^{1/v_i} = \sinh\tau_{max}[1 + \Lambda] - \tau_{max} = B_0 \tag{20}$$

where

$$\Lambda = \frac{2G^2\beta\alpha}{\left[\ln\dfrac{2\sinh\tau_{max}}{\gamma'}\right]^3} \quad \text{and} \quad B_0 = \sinh\tau_0 - \tau_0$$

Generally, Λ turns out to be very small compared to 1; within the acceptable approximation $\Lambda \ll 1$, the maximum stress depends on only two parameters I and B_0

$$\sinh\tau_{max} - \tau_{max} = \mathrm{I} + B_0 \tag{21}$$

where

$$\mathrm{I} = G^2\beta\alpha\gamma' v_i^3 e^{1/v_i} \tag{22}$$

Aside from B_0, which is found to be generally much less than I, all the parametric dependence is contained in the single nondimensional quantity I.

To compare the approximate solution, equation (21), with the results of the full numerical solutions of equations (9) and (10), equation (21) is also plotted on Figs 2–4 as a function of several individual parameters. In addition, the nondimensional maximum stress is plotted against the dimensionless parameter I in Fig. 5.

Using the results of the approximation $\Lambda \ll 1$, one can calculate Λ. At very low dimensionless strain-rates ($\gamma' \approx 10^{-8}$), $\Lambda \ll 1$ is an excellent approximation. For very large dimensionless strain-rates ($\gamma' \approx 10^{-2}$), Λ can be 0.27 or larger, but because of the logarithmic dependence at high stresses, its relative effect is small. B_0 is generally less than 1, and therefore only contributes at very low dimensionless strain-rates.

Limiting cases of equation (21) provide additional insight into the dependence of the maximum stress on physical parameters. For τ_{max} large, equation (21) becomes

$$\tau_{max} = \ln[2(\mathrm{I} + B_0)] \tag{23}$$

while for τ_{max} small

$$\tau_{max} = [6(\mathrm{I} + B_0)]^{1/3} \tag{24}$$

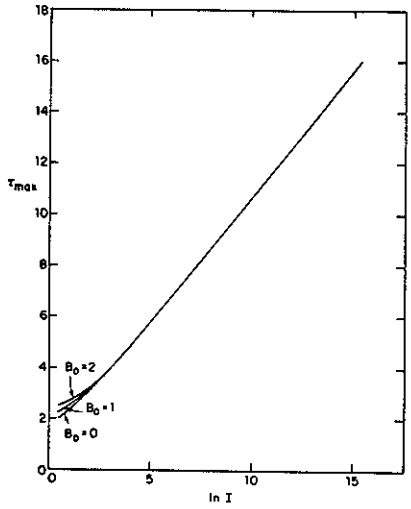

Fig. 5. Dependence of the nondimensional maximum stress on the nondimensional parameter I for several values of B_0 from equation (21) indicating an insensitivity to the free volume annihilation process.

5. SHEAR BAND ANALYSIS

A shear band analysis is now carried out with a geometry chosen to simplify the mathematics. Later, mention will be made of an analysis of a shear band inclined with respect to the tensile axis. As depicted in Fig. 6, a sample is subjected to shearing boundary conditions. The sample is homogeneous except for a thin band of volume fraction ρ (a typical value of 10^{-6} will be used) of weaker (less viscous) material lying parallel to the direction of shearing. This geometric configuration was also considered by Argon [11] in his study of localization.

Equilibrium requires that the only non-zero component of stress, denoted by τ, be uniform throughout the sample. The constitutive law must be satisfied inside and outside the band. In the nondimensional variables defined earlier, the constitutive equations are written as

$$\frac{\tau'}{G} + 2e^{-1/v_b}\sinh\tau = \gamma_b' \tag{25}$$

$$\frac{\tau'}{G} + 2e^{-1/v_0}\sinh\tau = \gamma_0' \tag{26}$$

where γ_b' and γ_0' are the strain-rates inside and outside the band, respectively, and v_b and v_0 are the free volumes inside and outside the band. The respective free volume equations are

$$\alpha v_b' = e^{-1/v_b}\left[\frac{\cosh\tau - 1}{G\beta v_b} - \frac{1}{n_D}\right] \tag{27}$$

$$\alpha v_0' = e^{-1/v_0}\left[\frac{\cosh\tau - 1}{G\beta v_0} - \frac{1}{n_D}\right] \tag{28}$$

The total strain-rate, γ_a', is equal to the volume weighted average of the strain-rates inside and outside the band, according to

$$\rho\gamma_b' + (1-\rho)\gamma_0' = \gamma_a' \tag{29}$$

The initial conditions are $v_b = v_{b_i}$, $v_0 = v_{0_i}$ and $\tau = 0$ at $t = 0$. v_{0_i} is the free volume at the glass transition temperature and v_{b_i} is a small fraction above v_{0_i}. The higher free volume in the band provides for a slight initial weakening (lower viscosity). The free volumes should never achieve values lower than their respective initial values (i.e., the as-quenched state is the most relaxed state the material is capable of achieving). This is enforced by requiring that when $v_b = v_{b_i}$ or $v_0 = v_{0_i}$, initially for example, equations (27) and (28) only be valid when the term in brackets is non-negative. A constant total strain-rate, γ_a', is imposed and the equations are simultaneously integrated numerically to find the stress, free volumes, and viscosities as a function of time (or macroscopic strain).

A plot of the shear strain in the band as a function of the applied strain is shown in Fig. 7 for a typical set of physical parameters. The catastrophic character of the strain localization is evident: the applied strain and the stress remain essentially constant as the strain and the free volume in the band rise rapidly. The

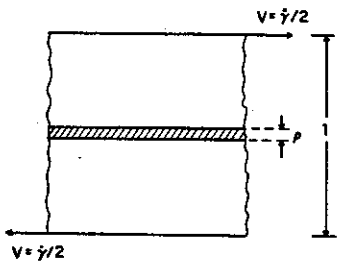

Fig. 6. Geometry for the shear band analysis.

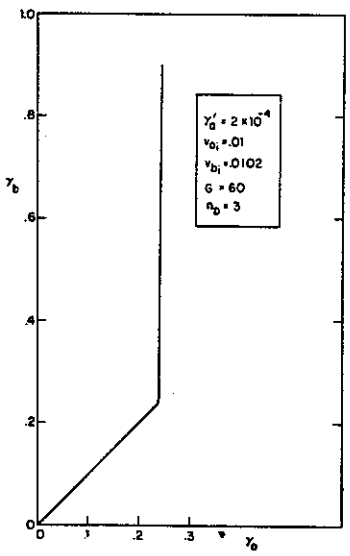

Fig. 7. Shear strain in the band as a function of the total shear strain.

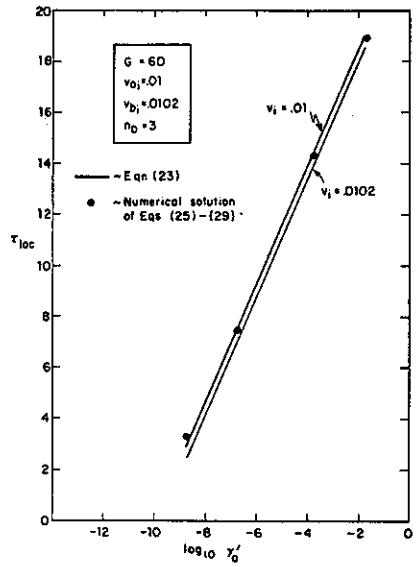

Fig. 8. Comparison of the localization stress with the stress at catastrophic softening for various values of the applied strain-rate.

points in Fig. 8 represent the stress at localization for several values of applied strain-rate.

To assess the accuracy of using the maximum stress (catastrophic softening) of a uniformly shearing sample as an estimate of the stress at the onset of localization, plots of the maximum stress as a function of strain-rate as given by equation (23) are also included in Fig. 8 (solid lines). The upper and lower curves correspond respectively to equating v_i with v_{0_i} and v_{b_i} of the comparable inhomogeneous sample. The near coincidence of the maximum stress with the localization stress indicates that localization hinges on the catastrophic softening due to free volume creation.

An analysis of a shear band inclined with respect to the tensile axis was carried out using the J_2 invariant to generalize the constitutive law to multiaxial stress states. All results continue to hold qualitatively and quantitatively regardless of the initial inclination of the shear band.

6. DISCUSSION

As mentioned in Section 2, Spaepen and Turnbull [18] have suggested that when inhomogeneous flow occurs the weakening which initiates the shear band is due to the stress concentration near microcracks which are inevitably present. The more tractable problem of strain localization in an initially weakened band in an infinite body has been considered here, however. The principal result is that equation (23), to a high degree of approximation, gives the stress at the onset of strain localization under conditions of constant applied strain-rate.

In what follows, the variation of the localization stress with temperature and strain-rate is investigated. When these variations are compared with results from tests carried out in the inhomogeneous flow regime, the simplified nature of the present model must be borne in mind. Furthermore, comparisons with theoretical models of steady state inhomogeneous flow are difficult because the stress at the onset of strain localization is considerably above the steady state flow stress (cf. Fig. 1) and has a very different dependence on parameters.

The flow properties are most concisely displayed on a deformation map [26–28], consisting of constant strain-rate contours plotted on axes of normalized stress and temperature. The deformation map in Fig. 9 shows the dependence of the localization stress on temperature for various values of strain-rate as given by equation (23).

Also plotted on the deformation map is an estimate of the curve below which no localization can occur. The following considerations allow an explicit expression for this curve to be derived. If the stress remained below the value τ_0 at which creation first exceeds annihilation no creation could occur, and hence the catastrophic softening necessary for strain localization would be precluded. The boundary curve is therefore given implicitly by equation (13). In fact, this is only a lower bound to the boundary curve. Although free volume creation occurs for pairs of stress and temperature above the curve shown, the softening may be insufficient (the stress relaxes before adequate rates of free volume creation are achieved) to cause localization.

It is noted that the localization stress is rather insensitive to temperature, consistent with experiments [8, 13]. Generally, the flow stress is observed to decrease slightly with temperature, whereas the present model predicts both increases and decreases. Furthermore, the localization stress is relatively strain-rate insensitive, as judged by the spacing of the strain-rate contours. The model does not predict,

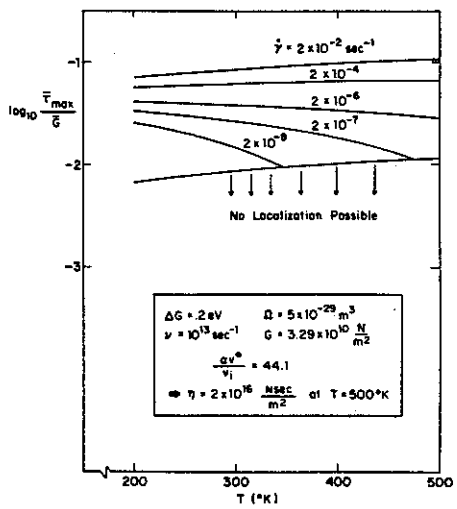

Fig. 9. Deformation map based on equation (23).

however, an almost ideally-plastic solid as Spaepen [1] and Argon [11] do on the basis of equations modelling steady state flow.

Formulae are now derived for the temperature coefficient and the strain-rate sensitivity of the localization stress. If the initial free volume, v_i, is also a function of temperature, the change with temperature of the localization stress as given by equation (23) is

$$\frac{\partial}{\partial T}\log\frac{\bar{\tau}}{\bar{G}} = \frac{1}{T}\left[1 - \frac{2 + \frac{\Delta G^m}{kT} + \frac{(1-3v_i)}{v_i^2}T\frac{dv_i}{dT}}{\tau_{max}}\right] \quad (30)$$

where τ_{max} is defined by equation (23). The localization stress rises or falls with temperature depending on whether the second term in the brackets in equation (30) is less than or greater than 1. The strain-rate, shear modulus, and certain other parameters influence the temperature coefficient through their effect on τ_{max}. Recent work by Taub and Spaepen [7, 10] on homogeneous flow suggests that even though a specimen is configurationally frozen, small reversible changes of free volume with temperature are possible. The term

$$T\frac{1-3v_i}{v_i^2}\frac{dv_i}{dT}$$

incorporates this effect, and it is always positive. Such a contribution would decrease the temperature coefficient but is not included in the results of Fig. 9.

The strain-rate sensitivity is equal to the inverse of the stress exponent given by

$$n \equiv \frac{\partial \ln \gamma'}{\partial \ln \tau} = \tau_{max} = \ln[2\beta\alpha G^2\gamma' v_i^3 e^{1/v_i}] \quad (31)$$

Equation (31) is plotted in Figure 10 as a function of strain-rate γ'.

As emphasized earlier, the present analysis is concerned only with the stress at the onset of localization.

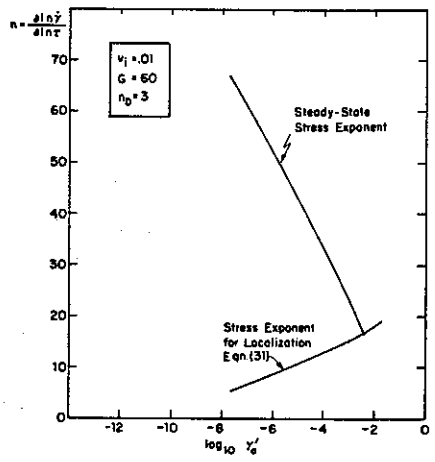

Fig. 10. Comparison of the steady state flow stress exponent with the stress exponent of the localization stress.

The localization stress deviates most widely from previous predictions of steady-state models in its strain-rate sensitivity. With the steady-state flow stress taken from Fig. 1, the steady-state strain-rate sensitivity may be calculated numerically. This has been done using the same parameters as above and is also plotted in Fig. 10. It is clear that the strain-rate sensitivity of the localization stress is very different from the present prediction of steady-state flow strain-rate sensitivity.

The present work gives insight into the variation of localization stress with physical parameters assuming the shear band is allowed to propagate freely across the specimen. An important qualitative result is evident from Fig. 3: a 50% decrease in the initial free volume of the sample leads to a twofold increase in the localization stress. Annealing of metallic glasses leads to decreases in free volume of this order [7]; the resultant increase in localization stress makes cleavage at a stress concentrator more likely. We are pursuing the implications of this effect on the brittle fracture mechanism. Furthermore, the lower bound to inhomogeneous flow, equation (13), provides an indication as to whether the deformation will localize or rather take place homogeneously with the sample slowly necking down.

Acknowledgements—This work was supported in part by the National Science Foundation under Grant DMR-79-23597, by the Office of Naval Research under Contract N00014-77-C-0002, and by the Division of Applied Sciences, Harvard University. P.S.S. also acknowledges the support of a National Science Foundation Predoctoral Fellowship.

REFERENCES

1. F. Spaepen, *Acta metall.* **25**, 407 (1977).
2. J. Megusar, A. S. Argon and N. J. Grant, *Proc. 3rd Int. Conf. on Rapidly Quenched Metals*, (edited by B. Cantor), p. 392. The Metals Society, London, (1978).
3. T. Murata, T. Masumoto and M. Sakai, *ibid.*, p. 401.
4. A. I. Taub, *Acta metall.* **28**, 633 (1980).
5. C. P. Chou and F. Spaepen, *Acta metall.* **23**, 609 (1975).
6. H. Kimura and T. Masumoto, *Acta metall.* **28**, 1663 (1980).
7. A. I. Taub and F. Spaepen, *Acta metall.* **28**, 1781 (1980).
8. F. Spaepen, *Proc. 3rd Int. Conf. on Rapidly Quenched Metals*, (edited by B. Cantor), p. 253. The Metals Society, London (1978).
9. F. Spaepen, *J. non-cryst. Solids* **31**, 207 (1978).
10. F. Spaepen, in *Physics of Defects*, (edited by J. P. Poirier and M. Kléman), Les Houches Lectures XXXV, North Holland, to be published.
11. A. S. Argon, *Acta metall.* **27**, 47 (1979).
12. H. S. Chen and D. E. Polk, *J. non-cryst. Solids* **15**, 174 (1974).
13. C. A. Pampillo, *J. Mater. Sci.* **10**, 1194 (1975).
14. L. A. Davis, in *Metallic Glasses*, (edited by J. J. Gilman and H. J. Leamy), p. 190. ASM, Metals Park, Ohio, (1978).
15. F. Spaepen, *Acta metall.* **23**, 615 (1975).
16. A. S. Argon and M. Salama, *Meter. Sci. Engng.* **23**, 219 (1976).
17. C. A. Pampillo, *Scripta metall.* **6**, 915 (1972).
18. F. Spaepen and D. Turnbull, *Scripta metall.* **8**, 563 (1974).

19. M. H. Cohen and D. Turnbull, *J. chem. Phys.* **31**, 1164 (1959).
20. D. Turnbull and M. H. Cohen, *J. chem. Phys.* **34**, 120 (1961).
21. D. Turnbull and M. H. Cohen, *J. chem. Phys.* **52**, 3038 (1970).
22. D. E. Polk and D. Turnbull, *Acta metall.* **20**, 493 (1972).
23. F. S. Gradshteyn and I. W. Ryzhik (Editors), *Table of Integrals, Series and Products* p. 93. Academic Press, New York (1965).
24. M. Abromowitz and I. A. Stegun (Editors), *Handbook of Mathematical Functions*, p. 228. National Bureau of Standards, Washington, D.C. (1964).
25. *ibid.*, p. 231.
26. M. F. Ashby, *Acta metall.* **20**, 887 (1972).
27. H. J. Frost and M. F. Ashby, *Proc. of the John E. Dorn Symposium*, (edited by J. C. M. Li and A. K. Mukherjee), p. 70. ASM, Cleveland, Ohio, (1975).
28. M. F. Ashby and H. J. Frost, in *Constitutive Equations in Plasticity*, (edited by A. S. Argon), p. 117. M.I.T. Press, Cambridge (1975).